Novel allele-dependent role for APOE in controlling the rate of synapse pruning by astrocytes

Won-Suk Chung[a,1], Philip B. Verghese[b,2], Chandrani Chakraborty[a], Julia Joung[a,3], Bradley T. Hyman[c,d], Jason D. Ulrich[b], David M. Holtzman[b], and Ben A. Barres[a,4]

[a]Department of Neurobiology, School of Medicine, Stanford University, Stanford, CA 94305; [b]Department of Neurology, Hope Center for Neurological Disorders, Charles F. and Joanne Knight Alzheimer's Disease Research Center, Washington University, School of Medicine, St. Louis, MO 63110; [c]Massachusetts Alzheimer Disease Research Center, Massachusetts General Hospital, Charlestown, MA 02129; and [d]Department of Neurology, Massachusetts General Hospital, Boston, MA 02129

Contributed by Ben A. Barres, June 20, 2016 (sent for review January 18, 2016; reviewed by Alison Goate and Rudolph Tanzi)

The strongest genetic risk factor influencing susceptibility to late-onset Alzheimer's disease (AD) is apolipoprotein E (*APOE*) genotype. APOE has three common isoforms in humans, E2, E3, and E4. The presence of two copies of the *E4* allele increases risk by ∼12-fold whereas *E2* allele is associated with an ∼twofold decreased risk for AD. These data put APOE central to AD pathophysiology, but it is not yet clear how *APOE* alleles modify AD risk. Recently we found that astrocytes, a major central nervous system cell type that produces APOE, are highly phagocytic and participate in normal synapse pruning and turnover. Here, we report a novel role for APOE in controlling the phagocytic capacity of astrocytes that is highly dependent on APOE isoform. APOE2 enhances the rate of phagocytosis of synapses by astrocytes, whereas APO4 decreases it. We also found that the amount of C1q protein accumulation in hippocampus, which may represent the accumulation of senescent synapses with enhanced vulnerability to complement-mediated degeneration, is highly dependent on *APOE* alleles: C1q accumulation was significantly reduced in *APOE2* knock-in (KI) animals and was significantly increased in *APOE4* KI animals compared with *APOE3* KI animals. These studies reveal a novel allele-dependent role for APOE in regulating the rate of synapse pruning by astrocytes. They also suggest the hypothesis that AD susceptibility of *APOE4* may originate in part from defective phagocytic capacity of astrocytes which accelerates the rate of accumulation of C1q-coated senescent synapses, enhancing synaptic vulnerability to classical-complement-cascade mediated neurodegeneration.

APOE allele | astrocytes | synapse elimination | phagocytosis | C1q

Alzheimer's disease (AD), the most common cause of dementia, is characterized clinically by a progressive and irreversible loss of cognitive functions. The neuropathological hallmarks of AD include profound synaptic loss and selective neuronal cell death, as well as the formation of extracellular amyloid beta plaques (Aβ) (1) and intracellular neurofibrillary tangles (2). Most cases of AD are the late-onset form, which develops after age 60. The causes of late-onset AD are not yet completely understood; however, genetic studies have shown that apolipoprotein E (*APOE*) alleles profoundly affect AD susceptibility, with *APOE4* being the major genetic risk factor. APOE, a 299-amino acid lipid transport protein, has three common isoforms in humans—APOE2 (Cys-112 and -158), APOE3 (Cys-112 and Arg-158), and APOE4 (Arg-112 and -158)—that are products of alleles at a single gene locus (3, 4). The *APOE3* is the most common and mediates intermediate risk for AD. The *APOE4* allele is significantly overrepresented in late-onset AD patients and has a dosage effect on the risk and age of onset of AD (5), whereas *APOE2* is protective against AD (6). Moreover, recent whole-genome sequencing of humans that age without developing diseases showed that there is a significant depletion of *APOE4* alleles in the healthy aging population (7). How do different APOE isoforms influence the age of onset and course of disease in AD? Although there is strong evidence that APOE isoform-dependent aggregation and clearance of Aβ play an important role in mediating AD risk (8–10), it has been also suggested that APOE may have Aβ-independent roles in the pathogenesis of AD. Transgenic mice expressing APOE4 in astrocytes have impaired working memory compared with those expressing APOE3 in astrocytes, despite the absence of significant Aβ deposition and plaque formation in the brains (11). Moreover, *APOE4* knock-in (KI) mice, in which mouse *ApoE* gene is replaced with human *APOE4*, develop spatial learning and memory deficits without Aβ accumulation (12–14). In agreement with the neuronal and behavioral deficits in *APOE4* KI mice, *APOE4* KI animals have significantly fewer dendritic spines compared with *APOE2* and *APOE3* KI animals (15). Therefore, different APOE isoforms may influence the risk for AD through synaptic structure and function independently, or collaboratively, with APOE's effect on Aβ.

Previously, we found a novel function of astrocytes in actively engulfing/eliminating synapses throughout the CNS (16). Specifically, by phagocytosing synapses through the Multiple EGF-like–domains 10 (MEGF10) and MER receptor tyrosine kinase (MERTK) phagocytic pathways, astrocytes actively contribute to the neural activity-dependent synapse elimination that mediates the refinement of neural circuits in the developing CNS. Developing mice deficient in both *Megf10* and *Mertk* pathways show a failure of the normal refinement of connections and, as a

Significance

Susceptibility to Alzheimer's disease (AD) is strongly controlled by apolipoprotein E (*APOE*) genotype. The *E4* allele greatly increases risk whereas the *E2* allele decreases risk, but it is not known how the *APOE* allele controls AD risk. In this paper, we report a novel role for APOE by showing that APOE2 enhances and APOE4 decreases the rate of synapse pruning and turnover in the brain by astrocytes. We also show that *APOE* alleles control the rate of accumulation of the complement C1q protein, which we hypothesize, reflects senescent synapse accumulation during normal brain aging and vulnerability of the aging brain to neurodegenerative diseases such as AD.

Author contributions: W.-S.C. and B.A.B. designed research; W.-S.C., C.C., and J.J. performed research; P.B.V., B.T.H., J.D.U., and D.M.H. contributed new reagents/analytic tools; W.-S.C. analyzed data; and W.-S.C. and B.A.B. wrote the paper.

Reviewers: A.G., Icahn School of Medicine at Mount Sinai; and R.T., Massachusetts General Hospital/Harvard Medical School (HMS).

The authors declare no conflict of interest.

[1]To whom correspondence may be addressed at the present address: Department of Biological Sciences, Korea Advanced Institute of Science and Technology, Daejeon, 34141, South Korea. Email: wonsuk.chung@kaist.ac.kr.

[2]Present address: C2N Diagnostics, Center for Emerging Technologies, 4041 Forest Park Avenue, Saint Louis, MO 63108.

[3]Present address: Broad Institute of MIT and Harvard, Cambridge, MA 02142; McGovern Institute for Brain Research, Department of Brain and Cognitive Science, Massachusetts Institute of Technology, Cambridge, MA 02139; and Department of Biological Engineering, Massachusetts Institute of Technology, Cambridge, MA 02139.

[4]To whom correspondence may be addressed. Email: barres@stanford.edu.

www.pnas.org/cgi/doi/10.1073/pnas.1609896113

result, retain excess functional synapses with their primary targets. Astrocytes were found to continuously engulf excitatory and inhibitory synapses in the adult CNS, suggesting that astrocytes may contribute to activity-dependent synapse turnover and homeostasis of the brain throughout life.

In this study, because APOE has been implicated in phagocytosis of cell corpses (17) and Aβ (18) in an isoform-dependent manner, we hypothesized that *APOE* alleles might also differentially control astrocyte-mediated synapse elimination in the brain.

Results

APOE-Dependent Synaptosome Uptake by Astrocytes. To test our hypothesis that the different APOE isoforms differentially control astrocyte-mediated phagocytosis, we first used a synaptosome-based in vitro engulfment assay (16) with astrocyte-conditioned medium (ACM) that contained secreted factors from astrocytes including APOE. ACM obtained from *APOE2*, *APOE3*, and *APOE4* homozygous KI astrocytes displayed a similar amount of protein secretion from astrocytes, but differed by their APOE isoforms. To create an APOE-free condition before APOE2/3/4 ACM addition, astrocytes from *ApoE* knockout (KO) animals were purified by the immunopanning method and cultured in a serum-free condition (19). After 3–5 d in vitro (DIV), tdTomato-positive synaptosomes were added in astrocyte cultures along with 1 or 5 μg of total protein from APOE2/3/4 ACM. Within 1 h, as expected, many of the tdTomato-positive synaptosomes were bound to astrocytes (Fig. 1*A*) and subsequently engulfed by phagocytosis (Fig. 1 *C* and *D*).

Surprisingly, when we measured the amount of bound synaptosomes per astrocyte after 1 h of incubation, we found that APOE2 ACM strongly enhanced binding of synaptosomes to astrocytes compared with APOE3 and APOE4 ACM (Fig. 1*B*). APOE4 ACM showed a minimum amount of associated synaptosomes with astrocytes among all ACMs, although the differences between APOE3 and APOE4 ACM were not statistically significant with the 1-h binding assay (Fig. 1*B*). Because this binding assay can be influenced by several factors, including force used for the washing step to dislodge unbound synaptosomes, we performed additional in vitro engulfment experiments with pHrodo-conjugated synaptosomes (16) that emit bright red fluorescence only after they get engulfed by astrocytes (Fig. 1 *C* and *D*) and localized in acidic organelles, such as lysosomes. This chemical pH indicator-based phagocytosis assay has been widely used because of its specificity and convenience for measuring the phagocytic activity (20–22). Compared with the negative control, adding pHrodo-conjugated synaptosomes significantly increased the astrocyte population with strong pHrodo intensity (Fig. 1*F*). Importantly, we found that APOE2 ACM significantly increased astrocyte-mediated synaptosome phagocytosis compared with APOE3 and APOE4 ACM (Fig. 1 *E* and *F*). Moreover, APOE4 ACM-treated astrocytes showed the lowest levels of phagocytosis (Fig. 1 *E* and *F*). Interestingly, *ApoE* KO ACM showed a similar level of phagocytosis to APOE3 ACM, suggesting that the absence of the endogenous mouse *ApoE* gene is not sufficient to trigger the changes in astrocyte-mediated phagocytosis (Fig. 1 *E* and *F*). Thus, the amount of synaptosome engulfment by astrocytes strongly depended on the human *APOE* allele.

APOE Particle-Dependent Synaptosome Uptake by Astrocytes. Although we could not detect differences in the amount of total proteins in each APOE2/3/4 ACM, *APOE2*, *3*, or *4* KI astrocytes could potentially produce different amount of APOE particles (23), as well as different sets of secreted proteins, affecting astrocyte-mediated phagocytosis. To test whether APOE2/3/4 molecules are directly responsible for differential phagocytic activities of ACM, we prepared lipidated recombinant apoE2, 3, and 4 particles and used these particles for our in vitro engulfment assay instead of ACM (24). APOE is secreted from astrocytes as unique high-density lipoprotein (HDL)-like lipoprotein particles that contain cholesterol, phospholipids, and other lipid classes. The majority of extracellular APOE exists as lipidated particles, and extensive biochemical studies have shown that lipid-free recombinant apoE proteins behave very differently (structurally

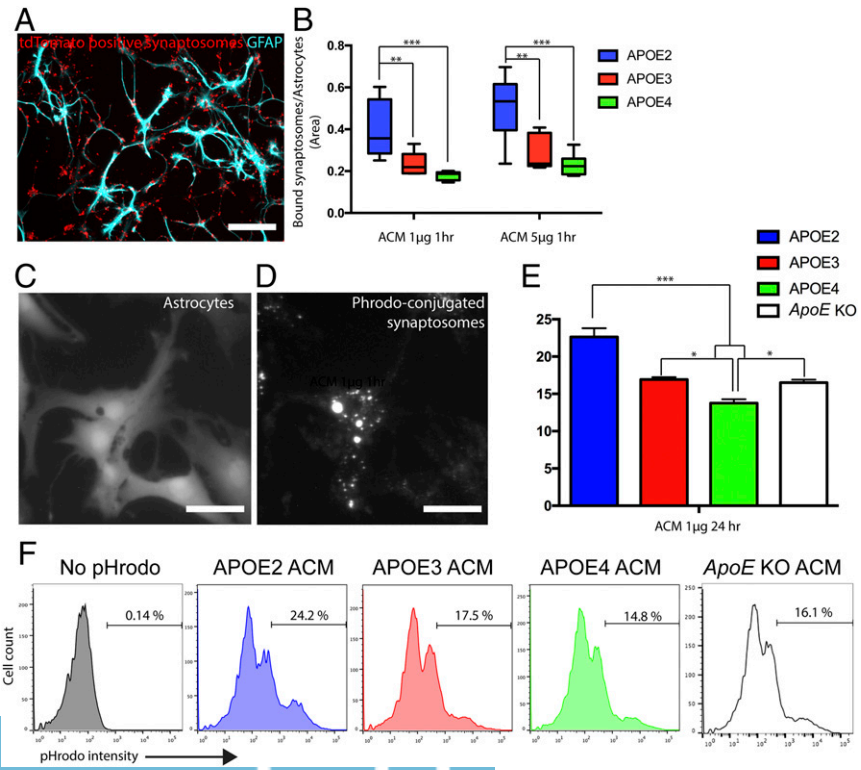

Fig. 1. APOE isoforms differentially control synaptosome engulfment by astrocytes. (*A*) In vitro binding assay with astrocytes (GFAP staining, cyan) and tdTomato-positive synaptosomes (red). (*B*) APOE2 ACM significantly enhances the binding between synaptosomes and astrocytes within 1-h incubation compared with APOE3 and APOE4 ACM. Note that APOE3 ACM always shows a higher value compared with APOE4, although it did not reach statistical significance in this 1-h binding assay. (*C* and *D*) In vitro engulfment assay with astrocytes (*C*) and pHrodo-conjugated synaptosomes (*D*). (*E*) Quantification of FACS data after the in vitro engulfment assay with ACM 1-μg treatment for 24 h. (*F*) Representative FACS analysis with APOE2/3/4 and *ApoE* KO ACM and pHrodo-conjugated synaptosomes. APOE2 ACM enhances and APOE4 reduces the number of astrocytes with high pHrodo intensity (>5 × 10^2 in pHrodo intensity) compared with APOE3 ACM. Representative data are from three independent experiments (*E* and *F*). $*P < 0.05$; $**P < 0.01$; $***P < 0.001$ (one-way ANOVA). Results are quantified and graphed ±SEM. [Scale bars, 50 μm (*A*) and 10 μm (*C* and *D*).]

and functionally) from the lipidated apoE, which is a biologically functional unit (25–28).

Because human CSF contains 150–300 nM APOE-containing lipoproteins, we added 200 and 400 nM apoE2, 3, or 4 lipidated particles along with pHrodo-conjugated synaptosomes into purified *ApoE* KO astrocytes and measured their phagocytic capacity by FACS. apoE2, 3, and 4 particles by themselves failed to show the differential effects on astrocyte-mediated phagocytosis that we have observed with the cognate ACMs (Fig. 2 *A* and *C*). These data suggest that other molecules in ACM might be required for eliciting APOE isoform-dependent phagocytosis. Astrocytes express several critical phagocytic receptors such as MEGF10 and MERTK, and mediate synapse elimination (16, 29). These receptors require opsonins, such as GAS6 and Protein S for MERTK (30), to bridge "eat-me signals" in the targets and phagocytic receptors in astrocytes (31). Therefore, we next repeated in vitro phagocytic assay with apoE2, 3, and 4 particles in the presence of opsonins (1 μg/mL Protein S). In the presence of Protein S, apoE2 particles significantly induced the phagocytic capacity of astrocytes compared with apoE3 particles, whereas apoE4 particles significantly reduced it (Fig. 2 *B* and *C*). These data imply that apoE2, 3, and 4 particles are not the direct inducers of phagocytosis, such as opsonins, but instead facilitate or inhibit the resident phagocytic pathways. Indeed, compared with Protein S, apoE2, 3, and 4 particles alone did not strongly induce synaptosome uptake by astrocytes (Fig. 2*D*). Astrocytes purified from postnatal day 7 (P7) WT rats and mice showed similar trends in responding to APOE2, 3, and 4 ACM and particles, suggesting that the effects of APOE2, 3, and 4 are dominant over WT mouse and rat ApoE.

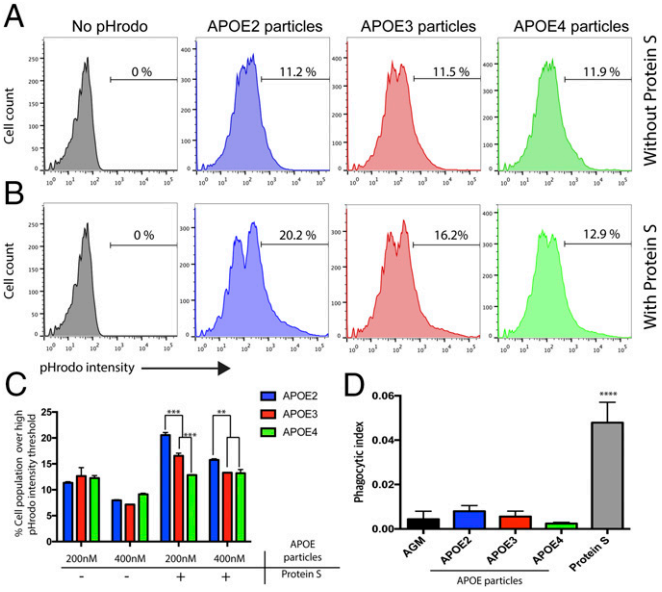

Fig. 2. APOE particles require opsonins to exhibit APOE isoform-dependent phagocytosis of astrocytes. (*A* and *B*) Representative FACS analysis with apoE2/3/4 particles and pHrodo-conjugated synaptosomes in the absence (*A*) and presence (*B*) of Protein S (1 μg/mL). (*A*) Without Protein S, apoE2/3/4 particles failed to show the difference in astrocyte-mediated phagocytosis. (*B*) With Protein S, apoE2 particles show an increase and apoE4 particles show a decrease in the number of astrocytes with high pHrodo intensity (>5 × 10^2 in pHrodo intensity) compared with apoE3 particles. (*C*) Quantification of FACS data. Note that high concentration (400 nM) of apoE particles actually reduced overall phagocytosis by astrocytes. (*D*) apoE2/3/4 particles alone do not induce significant phagocytosis compared with Protein S. Phagocytic index was calculated by measuring the area of pHrodo-positive synaptosomes normalized by area of astrocytes labeled by CFDA SE cell tracer kit. Representative data are from three independent experiments. $^{**}P < 0.01$; $^{***}P < 0.001$; $^{****}P < 0.0001$ (one-way ANOVA). Results are quantified and graphed ±SEM.

***APOE*-Dependent Synapse Elimination by Astrocytes in Vivo.** Because astrocytes in the developing CNS show robust phagocytic capacity and mediate activity-dependent synapse elimination during early postnatal development (16), we next investigated whether astrocytes in developing *APOE2*, 3, and 4 homozygous KI as well as *ApoE* KO CNS show differential phagocytic capacity. We outcrossed the *APOE2*, *APOE3*, and *APOE4* KI alleles and *ApoE* KO animals to an *Aldh1l1–egfp* transgenic line that expresses EGFP in all astrocytes in the mouse brain (29). To visualize synapse elimination by astrocytes, the contralateral eyes of homozygous KI or KO pups were injected with Alexa 594-conjugated cholera toxin-β subunit (CTB-594) to label axonal projections of retinal ganglion cells (RGCs), and WT siblings from the same crosses were used as controls. CTB-594 was injected at P4, and the animals were perfused at P6 to obtain the dorsal lateral geniculate nucleus (dLGN), a normal synaptic target zone of the RGCs. First, we found that the density of CTB-labeled RGC projections in the dLGN were comparable between all KI and KO animals, suggesting they have the similar amount of presynaptic terminals in the dLGN. By taking optical sections with confocal microscopy, we determined the phagocytic index (PI) of in vivo astrocytes by measuring the total volume of internalized CTB-594 (μm^3), normalized by the total volume of astrocytes (μm^3). In agreement with our in vitro engulfment assay, we found that astrocytes in *APOE2* KI animals showed significantly enhanced phagocytic capacity compared with *APOE3* and *APOE4* KI animals (Fig. 3), whereas astrocytes in *APOE4* KI animals showed a statistically significant decrease in phagocytic capacity compared with *APOE2* and *APOE3* KI animals (Fig. 3). Phagocytic capacity of *APOE3* KI astrocytes was comparable with that of astrocytes from mouse *ApoE* WT and KO animals, suggesting that *APOE2* and *APOE4* are dominant alleles over endogenous mouse *ApoE* (Fig. 3).

Together these data indicate that *APOE2* is a strong and *APOE4* a poor *APOE* allele in promoting synapse pruning and suggests the possibility that *APOE* allele-dependent AD susceptibility may arise, at least in part, by controlling the rate of astrocyte-mediated phagocytosis. In this hypothesis, *APOE2* could play a protective role for AD through efficient clearing of synaptic/neural debris by astrocytes, thus preventing accumulation of unwanted synapses/neural debris. Conversely, APOE4 could play a deleterious role for AD through inefficient clearance of synapses/neural debris, which can lead to defective synaptic turnover, accumulation of senescent synapses, and eventual synapse loss.

The Amount of C1q Accumulation in the Aging Brain Depends on *APOE* Allele. Our previous studies have demonstrated that a component of the innate immune system called the classical complement cascade helps to mediate normal developmental CNS synapse elimination (32). C1q, the initiating protein in the classical complement cascade, is localized to synapses and subsequently recognized/eliminated by phagocytic microglial cells expressing complement receptor, CR3 (33). In a mouse model of glaucoma, one of the most common neurodegenerative diseases, C1q becomes highly up-regulated and relocalizes to retinal synapses of RGCs at early stages of disease progression. Consistent with this finding, mice with a mutation in *C1q* are protected from glaucoma (34). Moreover, previous studies also have found that *C1q* protein level dramatically accumulates at the synapses in normal mouse and human aging brains (35) and is highly up-regulated in most or all neurodegenerative diseases, including AD (36) and dementia (37), where complement cascade components have emerged as significant enhancers of synapse vulnerability (37, 38). Together these data provide evidence that C1q is localized to senescent and diseased synapses and increases their vulnerability to any insults that would activate the complement cascade in the aging brain.

Because synapses are constantly turned over in the adult brains, we hypothesized that the different phagocytic capacity of astrocytes in *APOE2*, *3*, and *4* KI mice could contribute to the

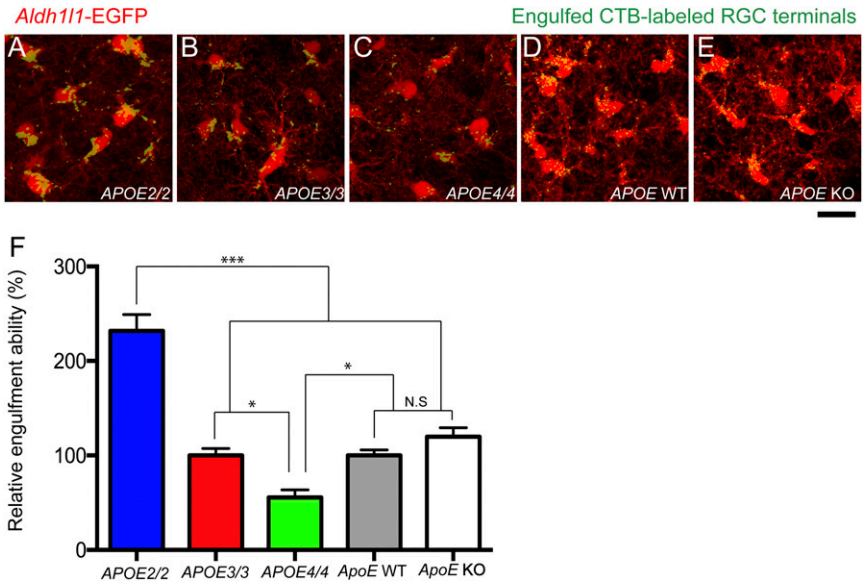

Fig. 3. Astrocytes in the developing brain show *APOE* allele-dependent phagocytic capacity. (*A–E*) In vivo engulfment assay of astrocytes in the developing retinogeniculate system showing astrocytes (Aldh1l1–EGFP, red) and engulfed CTB-594 labeled RGC projections (green) in *APOE2* (*A*), *APOE3* (*B*), and *APOE4* (*C*) homozygous KI animals as well as *ApoE* WT (*D*) and *ApoE* KO (*E*) animals. (*F*) Astrocytes in *APOE2* KI animals show a significant increase in relative engulfment ability compared with *APOE3* and *APOE4* KI animals. *APOE4* KI animals show a significant decrease in relative engulfment ability compared with *APOE3* KI animals. The phagocytic capacity of astrocytes between *ApoE* WT and KO animals is comparable. $n = 4$ mice per group. $^{*}P < 0.05$; $^{***}P < 0.001$; N.S., not significant (one-way ANOVA). Results are quantified and graphed ± SEM. [Scale bar, 20 μm (*A–E*).]

emergence and accumulation of C1q protein in normal brain aging. To test our hypothesis, we obtained 9- and 16-mo-old *APOE2*, *3*, and *4* homozygous KI mice and determined the C1q protein level in the hippocampus (Fig. 4 *A–C*) because we previously found that the hippocampus displays the earliest and highest level of C1q protein accumulation compared with other brain regions during normal aging (35). We found by immunostaining with a C1q-specific monoclonal antibody that there was a significant decrease in C1q protein level in *APOE2* KI animals compared with *APOE3* and *APOE4* KI animals in the 9- and 18-mo-old hippocampus (Fig. 4 *D* and *E*). In contrast, we detected a significant increase in C1q protein levels in the 18-mo-old *APOE4* KI hippocampus compared with *APOE2* and *APOE3* KI hippocampus (Fig. 4*E*). These changes in C1q protein levels are mainly due to the accumulation of C1q proteins in the brains because mRNA expression of C1q was not changed between *APOE2/3/4* KI hippocampus in any given ages (35). These data link *APOE* allele to the amount of C1q accumulation in the hippocampus with normal brain aging, with APOE4 enhancing C1q accumulation and APOE2 decreasing it.

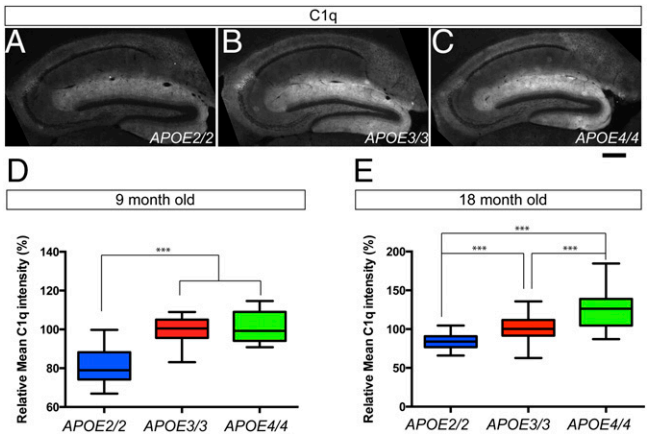

Fig. 4. Aged *APOE2/3/4* KI animals exhibit different levels of C1q protein accumulation in the hippocampus. (*A–C*) Representative images from C1q immunohistochemistry in the 9-mo-old hippocampus from *APOE2* (*A*), *APOE3* (*B*), and *APOE4* (*C*) homozygous KI animals. (*D*) In the 9-mo-old hippocampus, C1q accumulation is significantly reduced in *APOE2* KI animals compared with *APOE3* and *APOE4* KI animals. $n = 4$ mice per group. (*E*) In the 18-mo-old hippocampus, C1q protein accumulation is significantly reduced in *APOE2* KI hippocampus and significantly increased in *APOE4* KI hippocampus compared with *APOE3* KI hippocampus. $n = 4$ mice per group. $^{***}P < 0.001$ (one-way ANOVA). Results are quantified and graphed ±SEM. [Scale bar, 250 μm (*A–C*).]

Discussion

***APOE* Allele Significantly Controls the Rate of Synapse Pruning by Astrocytes.** Our findings demonstrate that different *APOE* alleles can differentially control the rate of astrocyte-mediated phagocytosis, such that APOE2 potentiates and APOE4 prevents efficient synapse elimination by astrocytes in vitro and in vivo. These findings reveal a novel allele-dependent role for APOE and provide a new hypothesis about how the *APOE* allele affects vulnerability to AD. The current efforts in tackling AD has been mostly focused on preventing the accumulation of Aβ or modulating the pathophysiology observed inside of neurons such as tauopathy (2). Because our data showed that *APOE* alleles modulate the phagocytic capacity of astrocytes, our findings suggest the possibility that initiation and/or progression of AD can be attributed, at least in part, to astrocytes. Moreover, the effects of APOE on astrocyte-mediated synapse elimination may also contribute to previously described *APOE* allele-dependent changes in synaptic plasticity, learning, and memory formation (39).

How Does the *APOE* Allele Control Astrocyte-Mediated Synapse Elimination? Our data showed that apoE2/3/4 particles are not sufficient to trigger synapse phagocytosis by astrocytes. Opsonins for astrocyte phagocytic pathways needed to be present for *APOE* isoforms to exhibit their differential control over phagocytosis. Astrocytes express a variety of phagocytic receptors—such as MEGF10, MERTK, AXL, INTEGRIN α5β5, and LRP1—and opsonins—such as GAS6, Protein S, and MFGE8 (29). Thus, APOE isoforms likely increase or decrease phagocytic rate by modulating one or more phagocytic pathways. This effect could be mediated by controlling binding affinity of the synapses/synaptic debris to their astrocyte receptors, and not through differential gene regulation, because we observed that APOE could elicit changes in binding between synaptosomes and astrocytes within 1 h. APOE could potentially help bridge the synapses/synaptic debris to the astrocyte surface by binding to APOE receptors present on the synapses and/or the astrocytes. Neurons have already been reported to express a variety of APOE receptors.

Similarly, our transcriptome analysis of astrocytes has found that astrocytes express a variety of APOE receptors, including LRP1, LRP8, LDLR, and VLDLR (29). Indeed, it was the very high level of expression of LRP1 by astrocytes, nearly as high as GFAP expression, that initially caused us to test the effects of APOE on phagocytic rate because LRP1 is a known phagocytic pathway receptor (40). APOE is also implicated in phagocytic clearance control. The *Drosophila* homolog of *APOE*, apolipophorin III, has been found to stimulate phagocytosis by fly macrophages (41). Moreover, *ApoE*-deficient mice exhibit a Draper/MEGF10 mutant-like defect in clearing severed axons after fimbria-fornix transection (42). Thus, it is possible that APOE receptors on astrocytes directly or synergistically enhance phagocytosis. Although this study is focused on the phagocytic capacity of astrocytes, it would be interesting to test whether microglia-dependent phagocytosis is also controlled by human *APOE* alleles because microglia expresses many of the APOE receptors (29). Furthermore, it will be important in future experiments to identity whether the relevant APOE receptor is one of the already known APOE receptors or a novel one.

Tentative Model for AD Susceptibility. How might the strong effects of APOE2 and APOE4 on enhancing and inhibiting the rates of astrocyte-mediated phagocytosis contribute to susceptibility to AD? In the mammalian eyes, when retinal pigment epithelia fail to clear the outer segment of photoreceptors because of the mutation in the TAM receptor pathways including MERTK, the uncleared membranes accumulate and induce the total degeneration of photoreceptors (43). Similarly, in the brain, where synapses are constantly formed and eliminated throughout development and adulthood, a sufficient rate of synapse turnover may be critical for synaptic health. Our recent studies on aging brain identified C1q as a protein that accumulates at CNS synapses in mouse and human by ∼300-fold during normal brain aging (35). Moreover, a recent study has shown that the profound loss of synapses at the early stages of AD could be prevented by blocking activation of the complement cascade (38). These findings suggested the possibility that C1q is accumulating because it is being bound by "senescent" synapses that accumulate in aging and that this accumulation is at least in part responsible for enhancing vulnerability of the aging brain to AD.

Our data provide evidence that APOE isoforms strongly control the rate at which C1q protein accumulates with brain aging. APOE2, a protective allele against AD, enhances the phagocytic capacity of astrocytes. The decreased C1q accumulation observed in the aged *APOE2* KI animals supports the hypothesis that APOE2 helps to maintain the synaptic environment clean from senescent synapses and aberrant immune reaction. In contrast, APOE4 decreases the overall phagocytic capacity of astrocytes, which leads to the more rapid accumulation of senescent synapses and their debris. APOE isoforms may similarly strongly control the rate by which astrocytes and microglia help to clear amyloid plaque accumulation.

Importantly, C1q accumulation at synapses is not sufficient to trigger their degeneration, because another signal is required to activate the complement cascade, culminating in removal of the complement-coated synapses by microglia (33). Oligomeric Aβ is a sufficient signal to trigger this cascade. In addition, other "second" hits may potentially activate the cascade at synapses. Accumulation of senescent synapses and their debris in the aged brain may induce reactive gliosis and neuroinflammation, and eventual synapse loss, an early pathophysiological aspect of AD patients. Whether decreasing phagocytic capacity of astrocytes by deleting astrocyte-specific phagocytic receptors could induce AD-like phenotypes in the brain, and whether increasing phagocytic capacity of astrocytes could prevent synaptic and behavior abnormalities in *APOE4* KI and AD mouse models, will be important questions for future study.

Materials and Methods

Animals. *APOE2* (B6.129P2-*Apoe*$^{tm1(APOE*2)Mae}$ N9), *APOE3* (B6.129P2-*Apoe*$^{tm2(APOE*3)Mae}$ N8), and *APOE4* (B6.129P2-*Apoe*$^{tm3(APOE*4)Mae}$ N8) KI mice were obtained from Taconic. *ApoE* KO mice (B6.129P2-*Apoe*^{tm1Unc} /J) were purchased from the Jackson Laboratory. *Aldh1l1–EGFP* (29) was used to visualize astrocytes. All lines were maintained by breeding with C57BL/6 mice. All procedures were approved by the Stanford University Administrative Panel on Laboratory Animal Care under Protocol 10726.

Synaptosome Purification. Synaptosomes were purified by Percoll gradient from the adult mouse brains as described (44). To obtain red fluorescent synaptosomes, the *Gt(ROSA)26Sor*$^{tm9(CAG-tdTomato)Hze}$*/J* line from the Jackson Laboratory was crossed to the ubiquitous *cre*-line (heat shock promoter driven *cre*-line), and the tdTomato-expressing adult brains were used for purifying synaptosomes. To obtain pHrodo-conjugated synaptosomes, synaptosomes purified from the WT adult brains were incubated with pHrodo Red and succinimidyl ester (Invitrogen) in 0.1 M sodium carbonate (pH 9.0) at room temperature with gentle agitation (45). After 2-h incubation, unbounded pHrodo was washed-out by multiple rounds of centrifugation, and pHrodo-conjugated synaptosomes were resuspended with isotonic buffer (pH 7.4) containing 5% (vol/vol) DMSO for subsequent freezing.

ACM. P1 *APOE2/3/4* KI mouse cortices were used to obtain and culture McCarthy and de Vellis (MD)-astrocytes as described (46). MD-astrocytes were plated on a 10-cm plate and cultured with medium containing 10% FCS. After 3 DIV, old medium was replaced with conditioning medium [50% neurobasal, 50% DMEM without phenol red, glutamine, pyruvate, *N*-acetylcysteine (NAC), and penicillin–streptomycin], and MD-astrocytes were cultured for an additional 3 d to enrich secreted factors from astrocytes. Any dead cells and debris were removed by centrifugation. Collected ACMs were further concentrated (×100) by Vivaspin protein concentrator spin columns (molecular weight cutoff 3,000; GE) and stored at 4 °C until being added to in vitro engulfment assay.

Preparation and Characterization of Reconstituted APOE and Astrocyte-Secreted APOE Isoforms. Reconstituted apoE2/3/4 particles were prepared by a cholate dialysis method using APOE:palmitoyloleoylphosphatidylcholine:cholesterol molar ratios of 1:50:10 (47, 48). Samples of the reconstituted apoE particles were analyzed by gel filtration-FPLC and nondenaturing gradient PAGE. Equal amounts of apoE isoforms (6 μg) were loaded in each lane of 4–20% Tris·glycine gel for native–PAGE (100 V at 4 °C for 16 h). The migration pattern of lipoproteins was assessed by using a protein mixture of estimated hydrodynamic radii as a standard (GE/Amersham).

In Vitro Engulfment Assay with Astrocytes. Astrocytes were purified from ∼P4 to ∼P6 *ApoE* KO or WT mouse cortex or WT rat cortex and cultured in a serum-free condition as described (19). Astrocytes at 3 to ∼5 DIV were washed twice with PBS and incubated with appropriate medium (see below) containing either tdTomato-expressing or pHrodo-conjugated synaptosomes. In the case of tdTomato-expressing synaptosomes, after incubating with synaptosomes for 1 h, astrocytes were washed several times with PBS to get ride of unbound synaptosomes, fixed with 4% paraformaldehyde, stained with GFAP (DAKO), and imaged by Zeiss Observer by taking 10 images per well using a ×20 objective lens from random area of the 24-well plates. Bound synaptosomes per astrocytes was calculated by measuring the thresholded area of synaptosomes (associated with astrocytes), normalized by the thresholded area of GFAP-labeled astrocytes. In the case of pHrodo-conjugated synaptosomes and FACS analysis, after incubating with synaptosomes for 20 h, astrocytes were trypsinized, collected by centrifugation, and resuspended in Dulbecco's PBS containing 0.02% BSA. Live astrocytes were analyzed at room temperature by the LSR 2 analyzer at the Stanford Shared FACS Facility on the basis of their pHrodo expression intensity. The PI was calculated by measuring the percentage of the cell population showing strong pHrodo intensity ($>5 \times 10^2$ in pHrodo intensity).

For testing APOE2/3/4 ACM, the concentrated ACM containing either 1 or 5 μg of total proteins was added to astrocyte growth medium (AGM: 50% neurobasal, 50% DMEM, glutamine, pyruvate, NAC, and penicillin–streptomycin, and 5 ng/mL HBEGF) along with synaptosomes into astrocyte cultures. For testing apoE2/3/4 particles, 200 or 400 nM particles was added to AGM along with synaptosomes (with or without Protein S, 1 μg/mL; Abcam) into astrocyte cultures. To label live astrocytes, the CFDA SE Cell Tracer Kit (ThermoFisher) was used.

In Vivo Engulfment Assay. *Aldh1l1–EGFP* was used to visualize astrocytes in all in vivo engulfment assays. P4 pups were anesthetized with isoflurane and 1 μL of CTB conjugated with Alexa 594 (Invitrogen; 1 mg/mL in normal saline)

was injected into the contralateral eyes. After 2 d, mice were perfused with PBS followed by 4% paraformaldehyde, and brains were dissected, postfixed overnight at 4 °C, and transferred to 30% sucrose for 24 h. The 50-μm floating coronal sections that contained dLGNs were mounted on slide glasses and used for the analysis. All of the following imaging processes were performed blindly to the genotype. For each animal, the two most medial dLGNs were chosen. For each dLGN, two fields, the tip and medial portions of dLGN, were imaged by using a Zeiss LSM510 inverted confocal microscopy to obtain ∼50 to 70 consecutive optical sections with 0.3-μm interval thickness. Each z-stack contained ∼30 to ∼40 astrocytes, and a total of four z-stacks spanning ∼15 to ∼21 μm of the LGN were used for the analysis. FIJI was used to remove outliers (radius 2.0 pixels and threshold 20) from all channels and subtract the background from CTB images (rolling bar radius 50 pixels). An image-processing algorithm (MATLAB; MathWorks) was used to localize engulfed CTB-labeled debris by subtracting CTB-labeled projections outside of astrocytes. The PI was calculated by measuring the total volume of engulfed CTB-labeled debris normalized by the total volume of astrocytes in a given z-stack. Relative engulfment ability was calculated by normalizing the PI of experimental groups to the WT group, which was comparable with the *APOE3* KI group.

C1q Immunohistochemistry. The 9- and 18-mo-old *APOE2/3/4* homozygous KI mice were perfused with PBS followed by 4% paraformaldehyde. Brains were dissected, postfixed for 3 or 16 h at 4 °C, and transferred to 30% sucrose for 24 h. After embedding brain tissues with optimal cutting temperature compound, 30-μm tissue sections were prepared by Leica cryostats and stored in PBS at 4 °C. Rabbit anti-mouse C1q monoclonal antibody (clones 4.8 and 27.10 at 1.0 μg/mL; Epitomics/Abcam) (35), followed by appropriate secondary antibodies conjugated with Alexa fluorophore (Invitrogen), were used for staining floating brain sections. Images were acquired using Zeiss AxioImager fluorescence microscopy and C1q intensity levels were measured with FIJI. Relative Mean C1q intensity was calculated by normalizing the C1q fluorescent intensity of *APOE2* and *APOE4* KI hippocampus to that of *APOE3* KI hippocampus.

Data Analysis. All statistical analyses were performed by using GraphPad Prism 6 software.

Data were analyzed by one-way ANOVA followed by Turkey post hoc tests with 95% confidence.

ACKNOWLEDGMENTS. Part of the data were acquired at Stanford Neuroscience Microscopy Service, supported by NIH Grant NS069375. W.-S.C. was supported by NEI Career Transition Grant (K99) K99EY024690. This work was supported by NIH Grants 5 R21NS072556 (to B.A.B.), R01 NS090934 (to D.M.H.), and R01 AG047644; a McKnight Foundation Brain Disorder Award (to B.A.B.); an Ellison Foundation Senior Scholar Award (to B.A.B.); the JPB Foundation (B.A.B., D.M.H., and B.T.H.); and the BrightFocus Foundation (P.B.V.). This work was also supported by National Research Foundation of Korea Grants (funded by the Korean government) NRF-2016M3C7A1905391 and NRF-2016R1C1B3006969 (to W.-S.C.).

1. Selkoe DJ (2002) Alzheimer's disease is a synaptic failure. *Science* 298(5594):789–791.
2. Iqbal K, Liu F, Gong CX (2016) Tau and neurodegenerative disease: The story so far. *Nat Rev Neurol* 12(1):15–27.
3. Mahley RW (1988) Apolipoprotein E: Cholesterol transport protein with expanding role in cell biology. *Science* 240(4852):622–630.
4. Teter B (2000) Apolipoprotein E isotype-specific effects in neurodegeneration. *Alzheimers Rep* 3:199–212.
5. Corder EH, et al. (1993) Gene dose of apolipoprotein E type 4 allele and the risk of Alzheimer's disease in late onset families. *Science* 261(5123):921–923.
6. Corder EH, et al. (1994) Protective effect of apolipoprotein E type 2 allele for late onset Alzheimer disease. *Nat Genet* 7(2):180–184.
7. Erikson GA, et al. (2016) Whole-genome sequencing of a healthy aging cohort. *Cell* 165(4):1002–1011.
8. Holtzman DM, et al. (2000) Apolipoprotein E isoform-dependent amyloid deposition and neuritic degeneration in a mouse model of Alzheimer's disease. *Proc Natl Acad Sci USA* 97(6):2892–2897.
9. Koistinaho M, et al. (2004) Apolipoprotein E promotes astrocyte colocalization and degradation of deposited amyloid-beta peptides. *Nat Med* 10(7):719–726.
10. Dodart JC, et al. (2005) Gene delivery of human apolipoprotein E alters brain Abeta burden in a mouse model of Alzheimer's disease. *Proc Natl Acad Sci USA* 102(4): 1211–1216.
11. Hartman RE, et al. (2001) Behavioral phenotyping of GFAP-apoE3 and -apoE4 transgenic mice: apoE4 mice show profound working memory impairments in the absence of Alzheimer's-like neuropathology. *Exp Neurol* 170(2):326–344.
12. Raber J, et al. (1998) Isoform-specific effects of human apolipoprotein E on brain function revealed in ApoE knockout mice: Increased susceptibility of females. *Proc Natl Acad Sci USA* 95(18):10914–10919.
13. Raber J, et al. (2000) Apolipoprotein E and cognitive performance. *Nature* 404(6776): 352–354.
14. Bour A, et al. (2008) Middle-aged human apoE4 targeted-replacement mice show retention deficits on a wide range of spatial memory tasks. *Behav Brain Res* 193(2): 174–182.
15. Dumanis SB, et al. (2009) ApoE4 decreases spine density and dendritic complexity in cortical neurons in vivo. *J Neurosci* 29(48):15317–15322.
16. Chung WS, et al. (2013) Astrocytes mediate synapse elimination through MEGF10 and MERTK pathways. *Nature* 504(7480):394–400.
17. Grainger DJ, Reckless J, McKilligin E (2004) Apolipoprotein E modulates clearance of apoptotic bodies in vitro and in vivo, resulting in a systemic proinflammatory state in apolipoprotein E-deficient mice. *J Immunol* 173(10):6366–6375.
18. Castellano JM, et al. (2011) Human apoE isoforms differentially regulate brain amyloid-β peptide clearance. *Sci Transl Med* 3(89):89ra57.
19. Foo LC, et al. (2011) Development of a method for the purification and culture of rodent astrocytes. *Neuron* 71(5):799–811.
20. Fourgeaud L, et al. (2016) TAM receptors regulate multiple features of microglial physiology. *Nature* 532(7598):240–244.
21. Aziz M, Yang WL, Wang P (2013) Measurement of phagocytic engulfment of apoptotic cells by macrophages using pHrodo succinimidyl ester. *Curr Protocols Immunol* Chapter 14:Unit 14.31.
22. Colas C, et al. (2014) An improved flow cytometry assay to monitor phagosome acidification. *J Immunol Methods* 412:1–13.
23. Ulrich JD, et al. (2013) In vivo measurement of apolipoprotein E from the brain interstitial fluid using microdialysis. *Mol Neurodegener* 8:13.
24. Verghese PB, et al. (2013) ApoE influences amyloid-β (Aβ) clearance despite minimal apoE/Aβ association in physiological conditions. *Proc Natl Acad Sci USA* 110(19): E1807–E1816.
25. Ruiz J, et al. (2005) The apoE isoform binding properties of the VLDL receptor reveal marked differences from LRP and the LDL receptor. *J Lipid Res* 46(8):1721–1731.
26. Narita M, et al. (2002) Cellular catabolism of lipid poor apolipoprotein E via cell surface LDL receptor-related protein. *J Biochem* 132(5):743–749.
27. LaDu MJ, et al. (1994) Isoform-specific binding of apolipoprotein E to beta-amyloid. *J Biol Chem* 269(38):23403–23406.
28. LaDu MJ, et al. (1995) Purification of apolipoprotein E attenuates isoform-specific binding to beta-amyloid. *J Biol Chem* 270(16):9039–9042.
29. Cahoy JD, et al. (2008) A transcriptome database for astrocytes, neurons, and oligodendrocytes: A new resource for understanding brain development and function. *J Neurosci* 28(1):264–278.
30. Lew ED, et al. (2014) Differential TAM receptor-ligand-phospholipid interactions delimit differential TAM bioactivities. *eLife* 3:3.
31. Arandjelovic S, Ravichandran KS (2015) Phagocytosis of apoptotic cells in homeostasis. *Nat Immunol* 16(9):907–917.
32. Stevens B, et al. (2007) The classical complement cascade mediates CNS synapse elimination. *Cell* 131(6):1164–1178.
33. Schafer DP, et al. (2012) Microglia sculpt postnatal neural circuits in an activity and complement-dependent manner. *Neuron* 74(4):691–705.
34. Howell GR, et al. (2011) Molecular clustering identifies complement and endothelin induction as early events in a mouse model of glaucoma. *J Clin Invest* 121(4): 1429–1444.
35. Stephan AH, et al. (2013) A dramatic increase of C1q protein in the CNS during normal aging. *J Neurosci* 33(33):13460–13474.
36. Tenner AJ, Fonseca MI (2006) The double-edged flower: Roles of complement protein C1q in neurodegenerative diseases. *Adv Exp Med Biol* 586:153–176.
37. Lui H, et al. (2016) Progranulin deficiency promotes circuit-specific synaptic pruning by microglia via complement activation. *Cell* 165(4):921–935.
38. Hong S, et al. (2016) Complement and microglia mediate early synapse loss in Alzheimer mouse models. *Science* 352(6286):712–716.
39. Kim J, Yoon H, Basak J, Kim J (2014) Apolipoprotein E in synaptic plasticity and Alzheimer's disease: Potential cellular and molecular mechanisms. *Mol Cells* 37(11):767–776.
40. Gaultier A, et al. (2009) Low-density lipoprotein receptor-related protein 1 is an essential receptor for myelin phagocytosis. *J Cell Sci* 122(Pt 8):1155–1162.
41. Whitten MM, Tew IF, Lee BL, Ratcliffe NA (2004) A novel role for an insect apolipoprotein (apolipophorin III) in beta-1,3-glucan pattern recognition and cellular encapsulation reactions. *J Immunol* 172(4):2177–2185.
42. Fagan AM, et al. (1998) Evidence for normal aging of the septo-hippocampal cholinergic system in apoE (-/-) mice but impaired clearance of axonal degeneration products following injury. *Exp Neurol* 151(2):314–325.
43. Burstyn-Cohen T, et al. (2012) Genetic dissection of TAM receptor-ligand interaction in retinal pigment epithelial cell phagocytosis. *Neuron* 76(6):1123–1132.
44. Dunkley PR, Jarvie PE, Robinson PJ (2008) A rapid Percoll gradient procedure for preparation of synaptosomes. *Nat Protoc* 3(11):1718–1728.
45. Beletskii A, et al. (2005) High-throughput phagocytosis assay utilizing a pH-sensitive fluorescent dye. *Biotechniques* 39(6):894–897.
46. McCarthy KD, de Vellis J (1980) Preparation of separate astroglial and oligodendroglial cell cultures from rat cerebral tissue. *J Cell Biol* 85(3):890–902.
47. Matz CE, Jonas A (1982) Micellar complexes of human apolipoprotein A-I with phosphatidylcholines and cholesterol prepared from cholate-lipid dispersions. *J Biol Chem* 257(8):4535–4540.
48. Hime NJ, Drew KJ, Hahn C, Barter PJ, Rye KA (2004) Apolipoprotein E enhances hepatic lipase-mediated hydrolysis of reconstituted high-density lipoprotein phospholipid and triacylglycerol in an isoform-dependent manner. *Biochemistry* 43(38): 12306–12314.